Experimental Investigation of Flame Propagation during Fire Accidents in Confined Space

Cheeda V.K.

DDESC, Tirupati-101, Andhra Pradesh, India
Corresponding author's email: vijaya_cheeda_chanti@yahoo.co.in

ABSTRACT

Fire accidents in confined regions of public recreation theatres, malls, railroad cars and in tunnels are influenced by atmospheric, confinement and fuel charge conditions. Obstacles in the confinements are found to have a significant impact on flame propagation. Careful design of confinement geometry can avoid accidents or slow down the flame propagation. Current experimental investigation is intended to find the effect of obstacle interaction, free obstacle space, non-reacted gas flow, and turbulence at the near-wall on flame acceleration. Two rows of bench shaped obstacles enhance the flame speed in the obstacle free path. Turbulence intensity is higher in the local regions where flow is high subsonic and mildly supersonic, which enhances the flame speed.

KEYWORDS: Fire safety, confined space, obstacle spacing, turbulence intensity.

INTRODUCTION

Fire accidents in confined public places like auditoriums, schools and theaters, tunnels of mines, petro-chemical and fuel gas filling stations have become major cause of concern. At these places the risk involved of handling inflammable substances is high. The unintentional release of fuel gases during transportation in the confined and semi confined spaces has led to catastrophic consequences with life losses in the past. A few of such incidents are briefly discussed and summarized here. An incident of mishap at Port Hudson took place at Missouri in 1970 due to the outflow of propane gas from the transport pipe line into the open rural area. The gas cloud formed was ignited by an ignition source and established the detonation [1]. A fire accident at a large gasoline tank of Indian Oil Corporation depot in Jaipur, India (2009) was due to leakage of petrol from the transportation pipe line [2]; this fire damaged the depot. These types of incidents are classified as unconfined fire accidents. Fire broke out in Kumbakonam primary school, Tamilnadu (2004) from a charcoal grill and Upahar theater in Delhi (1997) due to coolant oil leakage from an electric transformer causing several fatalities. This explosion of the two phase gas-liquid fuel film led to the severe damage. Major reasons for such events were studied by Dabora EK et al [3], Roy GD et al [4] and Mitrofanov VV [5]. These incidents could lead to detonation which would cause much severe damage. In these incidents, the major cause of mortalities was found to be the toxic smoke. In the Upahar theater when the fire broke out, there was no provision for the smoke to escape, and the flame accelerated rapidly by chairs (obstacles) leaving no time to escape. These obstacles were found to increase the flame speed by many times, and this fast flame propagating in all directions caused great loss of life.

In addition, heavy toll was recorded in the accidents caused in rail and road tunnels. Fire accident in London tube at Kings Cross St. Pancras metro station (1987) was one such incident. Here carbon monoxide emission and smoke has increased the toll. The similar case is the Baku metro fire in

Proceedings of the Ninth International Seminar on Fire and Explosion Hazards (ISFEH9), pp. 321-332
Edited by Snegirev A., Liu N.A., Tamanini F., Bradley D., Molkov V., and Chaumeix N.
Published by St. Petersburg Polytechnic University Press
ISBN: 978-5-7422-6496-5 DOI: 10.18720/spbpu/2/k19-128

Azerbaijan (1995). Daegu subway fire accident in South Korea (2003) is another example. A Blaze set for Sabarmati Express train at Godhra, Gujarat (2002) by agitators has killed many people. The high causalities were reported due to fast flame, smoke and wedged doors due to distortion by rapid heat release. The chief reasons found in these incidents are inadequate provisions for safe escape from fire, faster disposal of smoke, improper design of systems and events enhancing the flame propagation. Among all the configurations of fire accidents, common reasons are leakages in storage tanks of inflammable materials, scattering of ignitable mixture of dust particles, confinement conditions, improperly placed obstacles (chairs in theaters, schools etc. [6]) and ignition source. In addition to sources of fire, the condition of flammable charge is also important. Although some of these cannot be eliminated, a well-designed system can minimize the loss. Therefore a prerequisite knowledge is required for a designer to reduce the risk and identify the methods to minimise accidents. Thus, the present investigation was carried out to determine various events which create fast flame. The results are presented in four sections. In the first part, experimental results of accelerating flame in confinement are discussed. The experiments are intended to examine the flame propagation mechanism and the gas dynamics effects. A miniature model (replicating transport carriers and auditoriums) was fabricated for the study. Accelerating flame in confinement compresses the stagnant air ahead of flame by volumetric expansion which causes the air to flow in the direction of the flame. This flow induce turbulence eddies. Such a flow phenomenon was elaborated in [7]. Thus to determine the turbulence intensity of the cold flow near the boundary layer and also in free stream zone, Laser Doppler velocimetry (LDV) measurements were performed. These results are presented in the second part of this paper. Salient cold flow features obtained from the numerical simulations are given in the third part. To investigate the similarity of gas dynamics effects in the mini model and the large scale flow structure, numerical simulations are performed for small and large room size geometries. These simulations are carried to complement the core investigation. The results are discussed separately in the appendix.

METHODOLOGY

The experimental model is shown in Fig. 1. A carpet made of cotton and paper spread on the bottom surface of the model. Sheet metal obstacles (objects) were placed which represent chairs. Several openings underneath the model acted as air circulating vents. Gasoline was spilled over carpet surface. The flame was initiated at the right bottom corner by a flash fire. A digital camera (Casio EX FH-20) was used to capture high speed images with an exposure time of 2.5e-5 s.

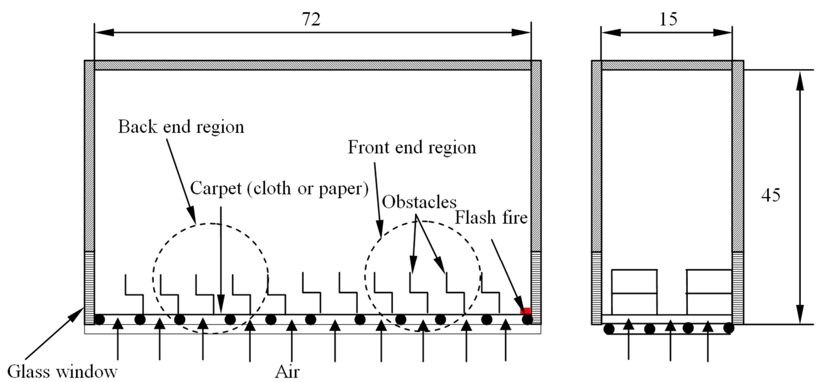

Fig. 1. Experimental setup for flame propagation in confined space (dimensions are in centimeters).

A glass window was used for optical access to record Schlieren and regular images. For the cold flow study, compressed air was admitted into the test setup from a reservoir through a gate valve at stagnation pressure of 3.5 bar (g). This pressure was maintained all through to obtain high subsonic flow in the test section. This flow condition was similar to that exists ahead of flame front. The run time was 10 s and simultaneously static pressure was measured by a transducer. The second test setup is shown in Fig.2.

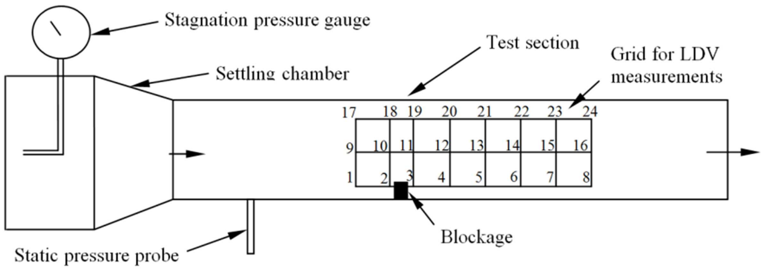

Fig. 2. Cold flow test setup for LDV measurements.

RESULTS AND DISCUSSION

Cloth carpet

High speed Schlieren images are shown in Fig. 3 (a). The images show that the flame accelerates faster when its edges has interacted with the obstacles. The flame propagates faster in the unobstructed path between the two rows of obstacles, Fig. 3 (b). The edges of the obstacles create the recirculation bubbles which mixed fuel vapour, air and product gas, thereby enabling faster burning. The single laminar flame front bifurcates into two fronts (F_1 and F_2) when flame interacts with the first two obstacles, Fig. 3 (b), which can be clearly seen in frame 3 and subsequent frames of Fig. 4. For large spacing (4 cm), two bifurcated flame fronts (separated by the first two obstacles) travel in the unobstructed flame path between the two rows of obstacles. Up to frame 5 of Fig. 4, the flame front is undisturbed, and it is perturbed later on. These perturbations can be seen in frames 10 to 12. The flame front engulfed the entire obstacle.

The reasons for these perturbations are the following.

1. Obstacle edges distort the flame surface.
2. Hot product gas and cold fuel vapour air mixture induced the Rayleigh Taylor (RT) instability (Fig. 5).
3. Interaction of cold air above flame surface and hot gases also causes the RT instability (Fig. 8).

The flame in the front end reaches above the height of the obstacles ($h_2 > h_1$). In the front end zone the flame encounters the obstacle bottom half first which distorted flame surface. Then for a length of 2.5 cm the flame does not distort. Later the top half of obstacle interacted upper surface of the flame which further deformed the flame. The delay in the expansion of the flame in the top surface caused curling which enhanced faster heat release. Apart from this, the bifurcated fronts travel in the lateral direction through the gap (two fronts in opposite direction). The gap is 2 cm on one side and 4 cm in middle between two the rows. The small gap yields slower flame and faster flame in the middle spacing (5 cm). Therefore this relative speed in flame fronts causes asymmetric lateral flamelets in the obstacle spacings in the same rows (Fig. 5). The opposite lateral flamelets from both sides lead to flame frontal collisions.

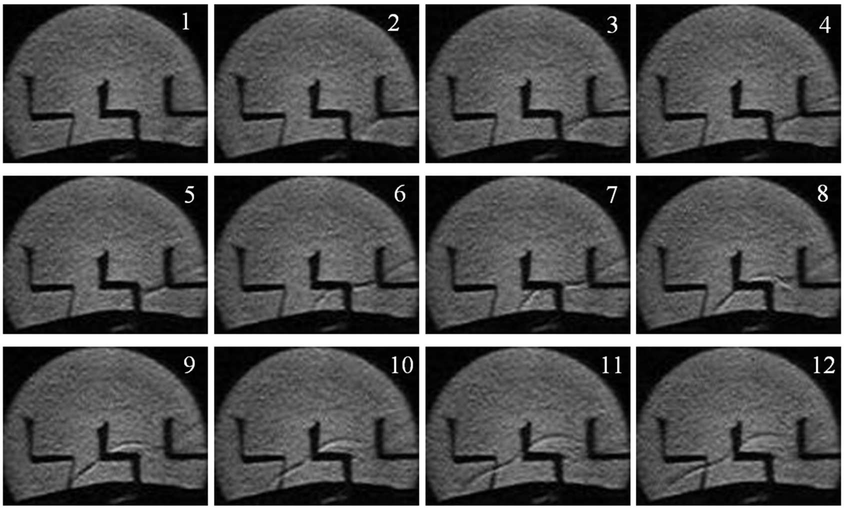

(a)

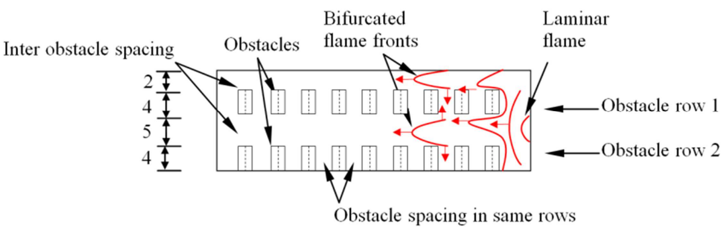

(b)

Fig. 3. (a) Spacing 2 cm back end cloth carpet. (b) Pictorial view of bifurcated flame fronts developed from laminar flame front.

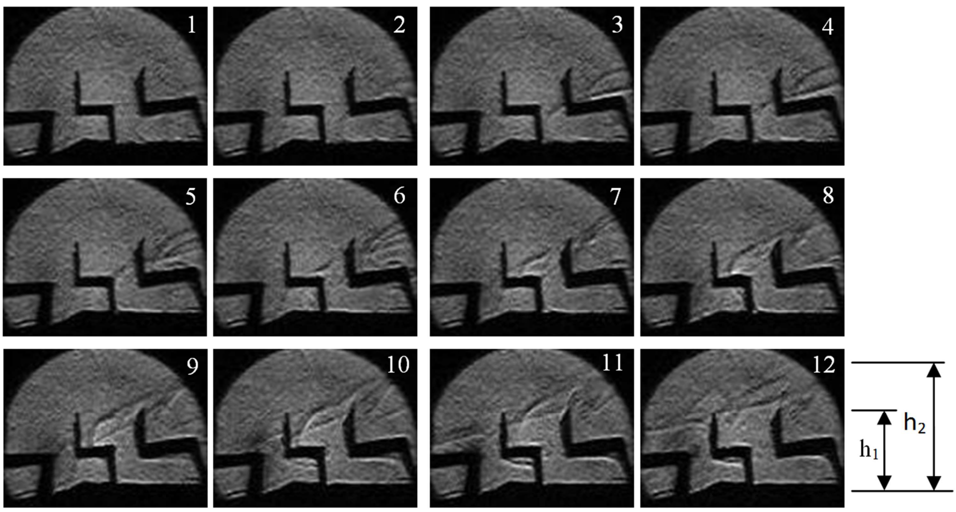

Fig. 4. Spacing 2 cm front end cloth carpet.

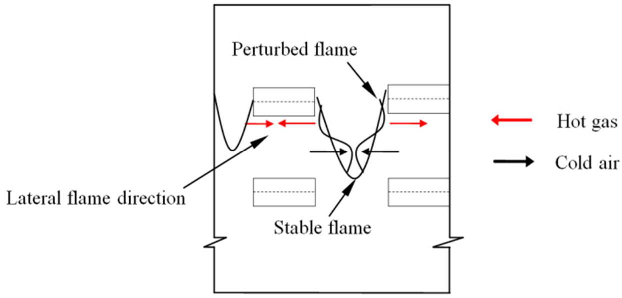

Fig. 5. Flame perturbations due to hydrodynamic instability (horizontal).

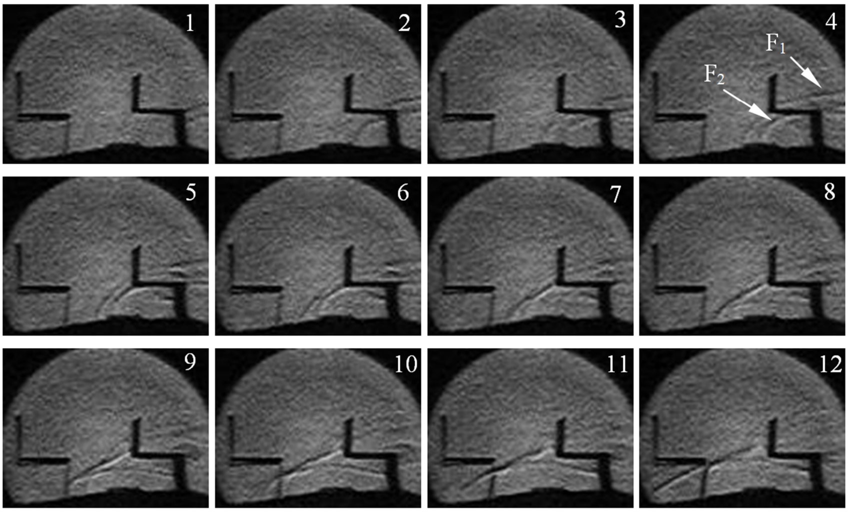

Fig. 6. Spacing 4 cm back end cloth carpet.

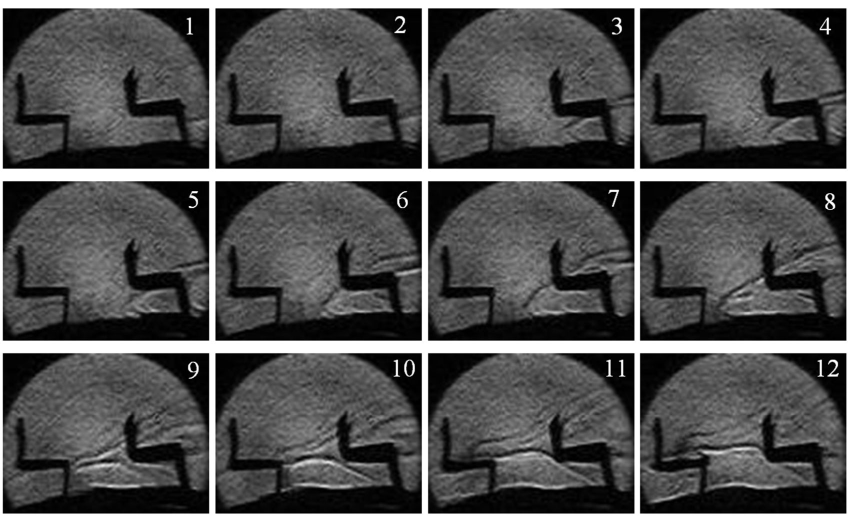

Fig. 7. Spacing 4 cm front end cloth carpet.

For large spacing of 4 cm, laminar bifurcated flames are obtained in the unobstructed inter obstacle space between the two obstacle laden rows. Up to the frame 5, the flame front is undisturbed. It becomes perturbed later on. The perturbations can be viewed in the frames 10 to 12 of Fig. 6. In the back end region, F_1 and F_2 are observed in one frame early. When the obstacles were separated by two centimeters more the flame acceleration was reduced.

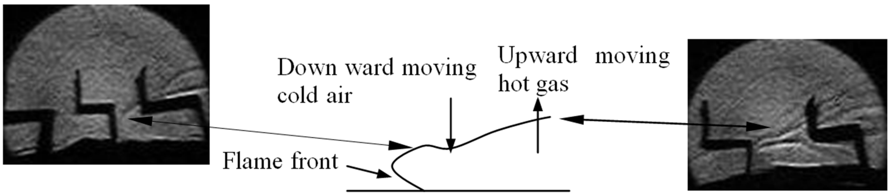

Fig. 8. Flame distortion due to buoyancy effect.

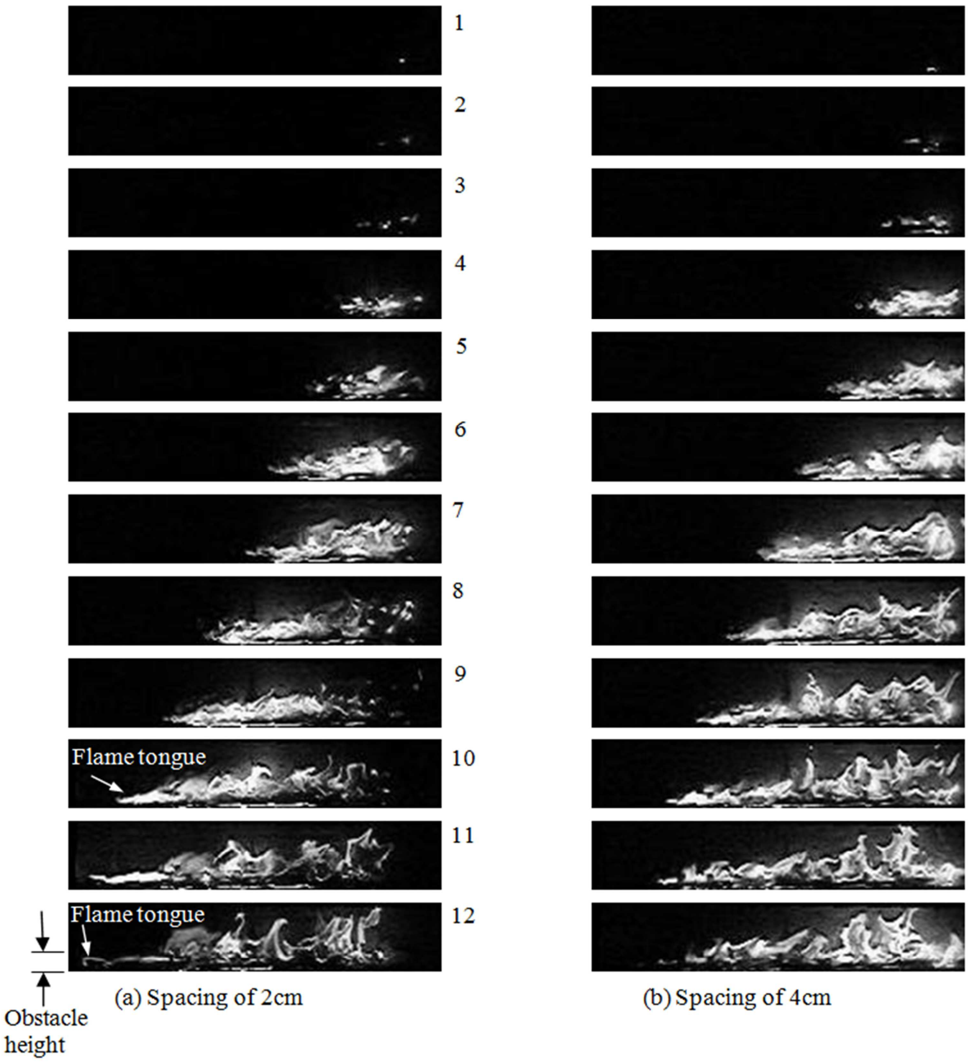

Fig. 9. Flame acceleration over the obstacles with cloth carpet.

However, the flame surface is less perturbed in the front end region (Fig. 7) compared to that in case of 2 cm separation (Fig. 4). In this region, the flame height merely approaches the obstacle height. Hot product gas moves upwards due to buoyancy, and cold air diffuses into the flame, thereby additionally distorting the flame surface (Fig. 8).

Flame kernel and laminar flame development can be observed in frames 1 to 3 of Fig. 9. Frames 4 to 9 show faster fuel consumption in 2 cm spacing (Fig. 9.a) but fuel burning is slower in 4 cm spacing (Fig. 9.b). Flame tongue is longer and faster when the obstacles were closely placed.

The turbulent scales become of order of obstacle height when the flame front crosses the objects. The flow of gas and air causes severe stretching in the flame surface. This effect results in the formation of flame tongue (Fig. 9 a).

Paper carpet

In spacing of 2 cm between obstacles with paper carpet flame front moves faster (Fig. 10) in back end region, where as in front end flame curling took place over the obstacles (Fig. 11). A vortex is generated on the flat surface of the obstacle (Fig. 11). For spacing of 4 cm, the flame slows down to a speed lower than that in the case of cotton carpet. Paper carpet does not absorb liquid fuel as the cotton does since the cotton fibres surface area is more thus more liquid is held due to surface tension. Therefore liquid film burns faster across the paper carpet. Small spacing between objects and mass diffusion of product gas and stream wise vortex caused additional enhancement for fast flame. The vortex promotes mixing of fuel vapor and product gas; thus, a faster burning is achieved. As a result, a faster heat release causes deformation in the sheet metal objects. In 4cm spacing in back end region, flame advancing is observed to be slower than in the case of 2 cm spacing (Fig. 12). When the flame is initiated at the rear side of the objects, vortex was not seen in the front end region (Fig. 13). The flame propagates faster when the spacing is 2 cm (Fig. 14). Therefore, the trend is similar to that of cotton.

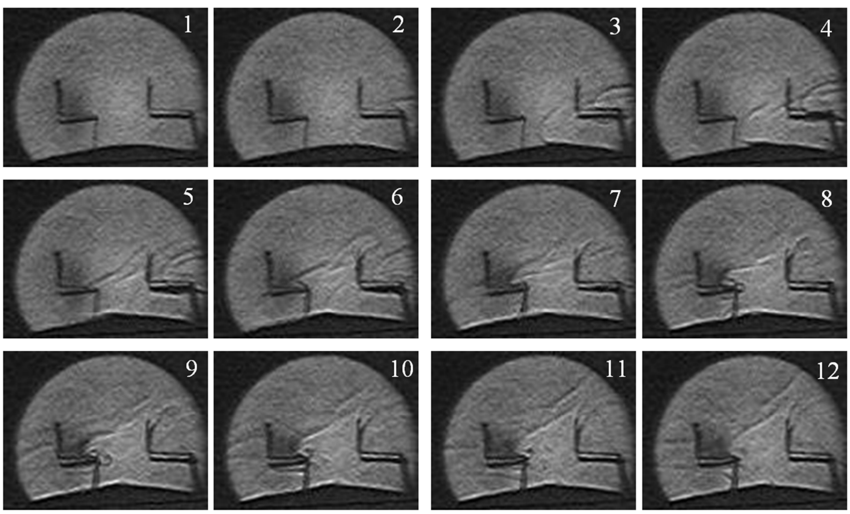

Fig. 10. Spacing 2 cm back end paper carpet

Cold flow investigation

Turbulence intensity in the flow was measured using LDV at different grid points as shown in Fig. 2 in a plane which was at 1 mm from the side wall. These grid points were separated by a spacing of 10 mm in upstream and downstream of obstacle. The grid spacing between leading and trailing edge of blockage was 5 mm. The grid points between 1 and 8 were at 6 mm from duct bottom wall and the points between 9 and 16 were at 18 mm from duct bottom wall. Grid points between 17 and 24 were located at 6 mm from top wall of the duct.

Highest turbulence intensity in the plane at 6 mm from bottom wall was obtained at grid point 6. The point 3 was located close to the trailing edge of the blockage. This point lies inside the shear layer. The point 6 was located near the shock wave, and the turbulence intensity was higher at these points due to the fluctuating shear layer. The range of turbulent intensity at different points in this plane is shown in Fig. 15. The turbulence intensity is higher at point 12, 15 and 16 in the middle plane (at the center of the duct). The points 15 and 16 are in regions of incident and reflected shock waves of the Mach stem shock wave. Intensity at these points is shown in Fig.16.

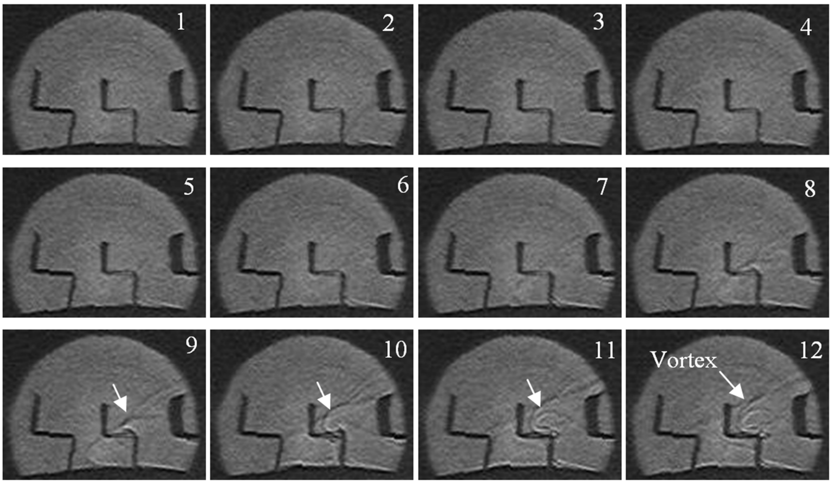

Fig. 11. Spacing 2 cm front end paper carpet.

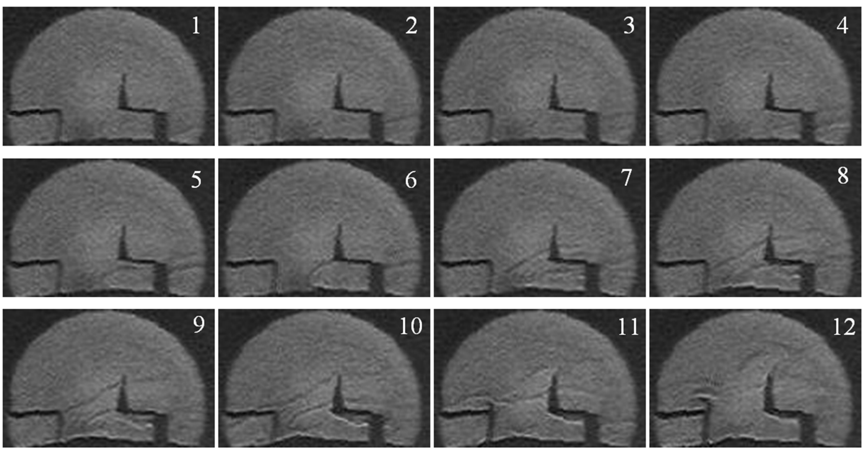

Fig. 12. Spacing 4 cm back end paper carpet.

The highest intensity near the top wall is at point 23 (Fig. 17) which is located in the normal shock region of Mach stem. The fluctuating shock waves and shear layer are causing highest turbulence intensities

CFD Results

Numerical simulations show higher intensity (calculated by k-ω model) in the region where boundary layers from bottom and side walls interact. Near the corner of two walls, the *k*-ω model predicts a higher fluctuating velocity. Outside the corner the intensity is higher in Reynolds Stress Model (RSM) results, as shown in Fig. 18 (a). The intensity is quite different outside the boundary layer in the symmetric plane, Fig. 18 (b). Overall turbulence intensity in the near wall and in the central regions is under-predicted by the *k*-ω model. The fine grid resolution and iterations are required in RSM compared to k-ω model [8]. The numerical calculations are compared with the experiments, and the results are in good agreement.

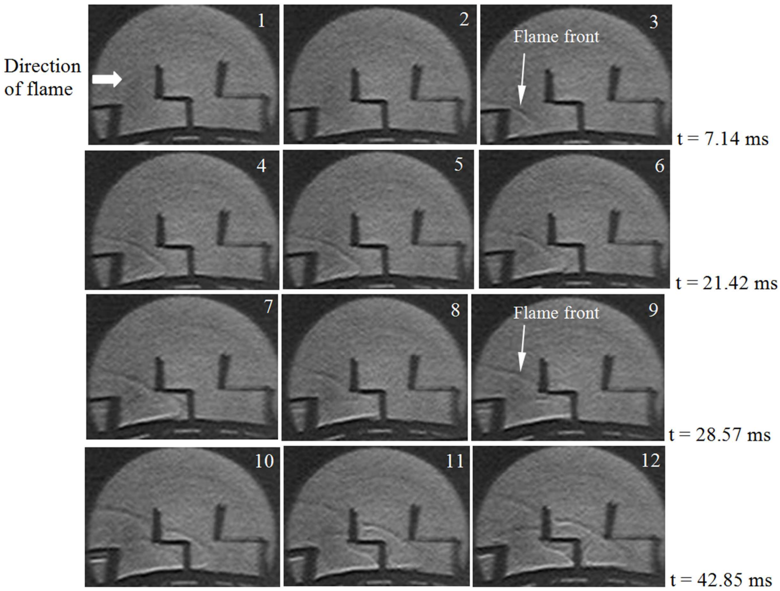

Fig. 13. Spacing 2 cm front end paper carpet (flame initiated from back side of the obstacles).

CONCLUSION

The present investigation indicates that the flame propagation in small scale models is influenced by inter-obstacle spacing. Flame propagates faster when spacing is of order of the obstacle size or when the obstacles are closely placed. Perturbations caused by the flow and hydrodynamic instability play vital role. Apart from this, the vortex generated between the closely placed objects promotes a faster flame. In addition, the cold flow experiments indicate the flow interaction with objects which locally form the shock waves or compression waves. Interaction of the flame front and these shocks produces more turbulence eddies, distorts the flame, and enhances its propagation. The LDV measurements show highest turbulence intensity in the near-wall region. RSM model calculations are better than *k*-ω model. Turbulence calculations show recirculations behind the objects which provide a better mixing of reactant and product gases. From the safety point of view, the chairs inter-obstacle spacing in transport carriers (automobiles and railway compartments) and public auditoriums should not be kept lower than the height of obstruction in order to avoid the fast flames and to minimise the losses.

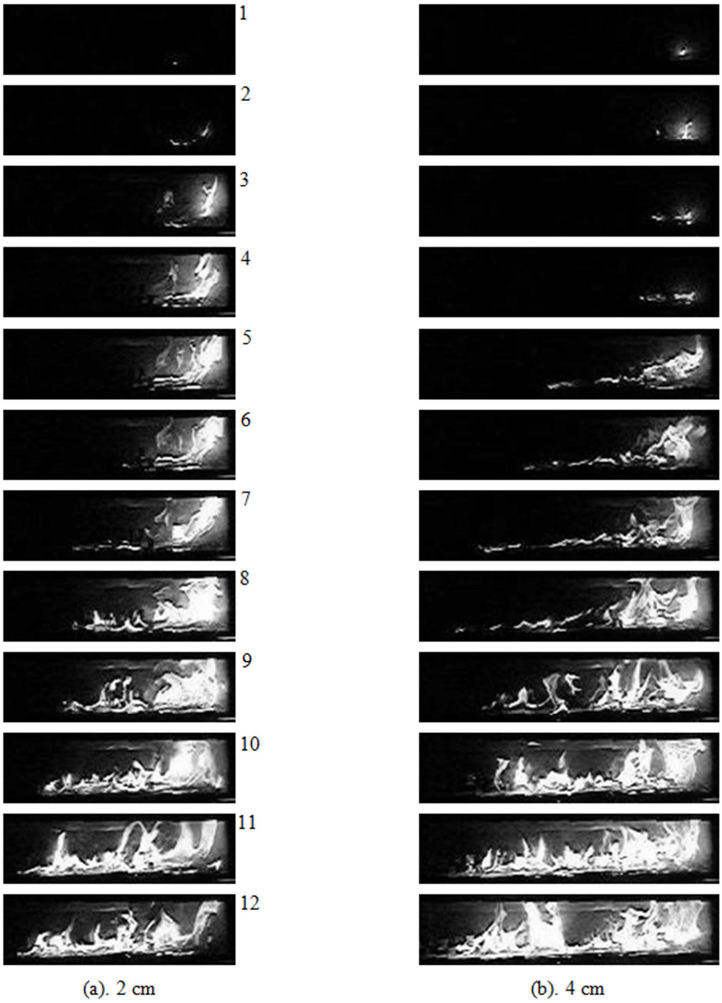

Fig. 14. Flame acceleration over the obstacles with paper carpet.

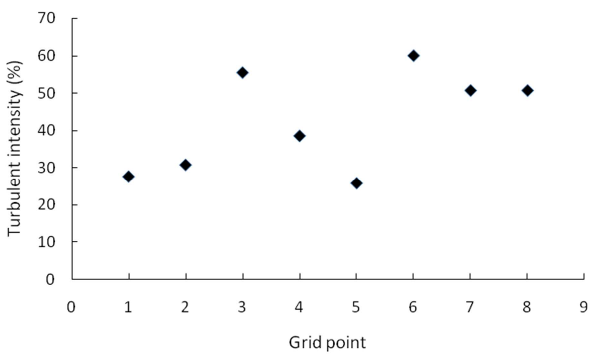

Fig. 15. Turbulence intensity at points between 1 and 8.

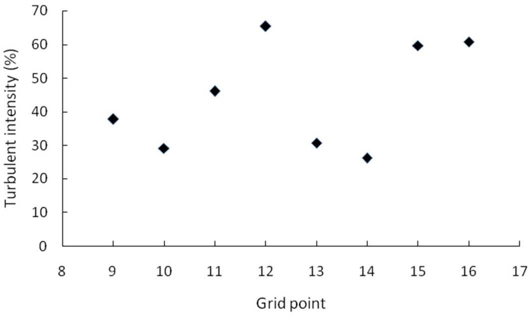

Fig. 16. Turbulence intensity at points between 9 and 16

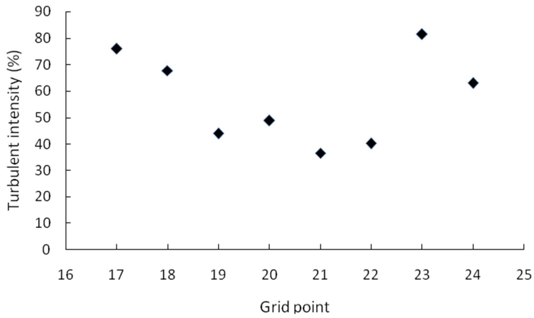

Fig. 17. Turbulence intensity at points between 17 and 24

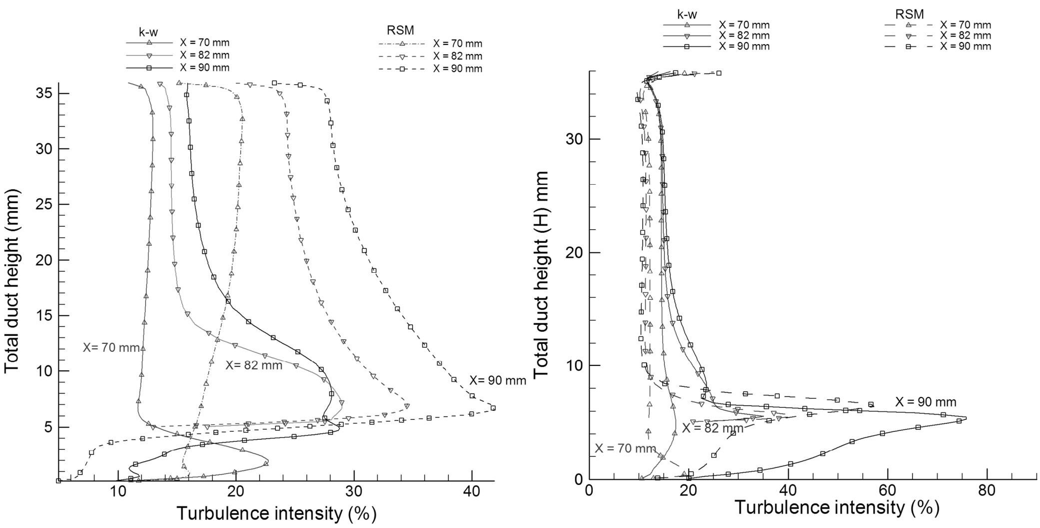

(a) (b)

Fig. 18. Turbulence intensity in Z-plane at (a) near side wall (0.5 mm) and (b) at the center of the duct.

REFERENCES

[1] D.S. Burgess, M.G. Zabetakis, Detonation of a flammable cloud following a propane pipeline break: the December 9, 1970, explosion in Port Hudson, Mo. (Technical Report BM-RI-7752), Bureau of Mines, Pittsburgh, Pa. (USA), Pittsburgh Mining and Safety Research Center, 1973.

[2] D.M. Johnson, Vapour Cloud Explosion at the IOC Terminal in Jaipur, Symposium Series No. 158, Hazards XXIII, Institution of Chemical Engineers, 2012.

[3] E.K. Dabora, L.P. Weinberger, Present status of detonations in two-phase systems, Acta Astronaut. 1 (1974) 361-372.

[4] G.D. Roy, S.M. Frolov, K. Kailasanath, N.N. Smirnov, Gaseous and Heterogeneous Detonations, Science for applications, Moscow, ENAS Publication, 1999, pp. 3-24.

[5] V.V. Mitrofanov, Theory of Detonations in Heterogeneous Media, Novosibirsk University Press, Novosibirsk, 1988.

[6] A.M. Na'inna, G. Somuano-Ballesteros, H.N. Phylaktou, G.E. Andrews, Flame Acceleration in Tube Explosions with up to Three Flat-bar Obstacles with Variable Obstacle Separation Distance, In: Tenth International Symposium on Hazards, Prevention, and Mitigation of Industrial Explosions (XISHPMIE) Bergen, Norway, 2014.

[7] V.K. Cheeda, Experimental Investigation of Interaction Shocks Formed in the Flow Field Behind Blockages, PhD Thesis, Indian Institute of Technology, Madras, India, 2016.

[8] S.M. El-Behery, M.H. Hamed, A Comparative Study of Turbulence Models Performance for Separating Flow, Comput. Fluids 44 (2011) 248-257.

APPENDIX

2D Numerical simulations are carried out to check the flow Mach number profile in miniature model height (H) of 36 mm and large size room (H = 3 m). Maximum flow Mach number in both geometries is plotted (Fig. A.1). This Mach number profile indicates similar trend in small and large ducts for blockage ratio below 0.5. For blockage ratios above 0.5 also the trend is same but the slopes are different. This exercise shows that the small scale experiments of flame acceleration would provide valid conclusions for large rooms.

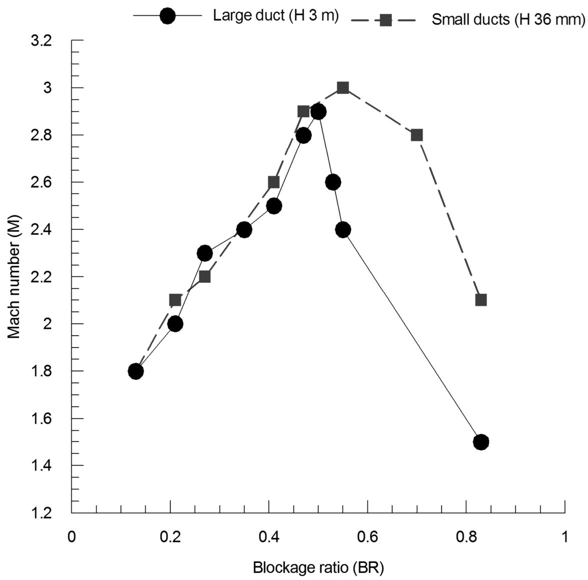

Fig. A.1. Maximum Mach number in small and large ducts.